Crossover from two- to three-dimensional behavior in superfluids

Norbert Schultka and Efstratios Manousakis
Department of Physics, Florida State University, Tallahassee, Florida 32306
(Received 2 June 1994; revised manuscript received 20 October 1994)

We have studied the superfluid density ρ_s on various size lattices in the geometry $L \times L \times H$ by numerical simulation of the x-y model using the cluster Monte Carlo method. Applying the Kosterlitz-Thouless-Nelson renormalization-group equations for the superfluid density we have been able to extrapolate to the $L \to \infty$ limit for a given value of H. In the superfluid phase we find that the superfluid density faithfully obeys the expected scaling law with H, using the experimental value for the critical exponent $\nu = 0.6705$. For the sizes of film thickness studied here the critical temperature $T_c^{2D}(H)$ is in agreement with the expected H dependence deduced from general scaling ideas.

I. INTRODUCTION

Liquid ^{4}He is an ideal experimental testing ground for the theory of phase transitions and the related finite-size scaling (FSS) theory. Relevant physical quantities such as the specific heat c or the superfluid density ρ_s can be measured to a very high accuracy[1–5] and they can be used to check the FSS theory (see, e.g., Ref. 6). This theory was developed in order to account for the influence of the finite extent of systems which are confined in a finite geometry (e.g., a film) and at temperatures close to the critical temperature. The theory is based on the scaling hypothesis and on the fact that finite-size effects can be observed when the bulk correlation length ξ becomes of the order of the relevant size of the system (e.g., in a film the relevant size is the film thickness H). More precisely, the finite-size scaling hypothesis states that a dimensionless physical quantity (or the ratio of two physical quantities of the same dimensions), sufficiently close to the critical point, is a function only of the ratio H/ξ. For a physical quantity O this simple but nontrivial statement can be expressed as follows:[7]

$$\frac{O(H,t)}{O(H=\infty,t)} = f\left(\frac{H}{\xi(H=\infty,t)}\right), \tag{1}$$

where t is the reduced temperature and f is a universal function. So far the validity of this approach has been confirmed by experiments on superfluid helium on helium films of finite thickness[2] (the relevant size is the thickness). However, recent measurements of the superfluid density by Rhee, Gasparini, and Bishop[3] of helium films seem to be in contradiction to the FSS theory.

The singular behavior in the thermodynamic functions of liquid ^{4}He close to the superfluid transition can be understood in terms of a complex order parameter $\psi(\vec{r})$ which is the ensemble average of the helium-atom–boson creation operator. This ensemble average is defined inside a volume of a size much greater than the interatomic distance but much smaller than the temperature-dependent coherence length. In order to describe the physics at longer length scales, which is important very close to the critical point, we need to consider spatial fluctuations of the order parameter. These fluctuations can be taken into account by assigning a Landau-Ginzburg free energy functional $\mathcal{H}(\psi(\vec{r}))$ to each configuration of $\psi(\vec{r})$ and performing the sum of $e^{-\mathcal{H}/k_BT}$ over such configurations. The power laws governing the long-distance behavior of the correlation functions and the critical exponents associated with the singular behavior of the thermodynamic quantities close to the critical point are insensitive to the precise functional form of $\mathcal{H}[\psi]$, and they are the same for an entire class of such functionals. The planar x-y model belongs to the class of such Landau-Ginzburg free-energy functionals,[8] and thus can be used to describe the fluctuations of the complex order parameter. In pseudospin notation the x-y model is expressed as

$$\mathcal{H} = -J \sum_{\langle i,j \rangle} \vec{s}_i \cdot \vec{s}_j, \tag{2}$$

where the summation is over all nearest neighbors and $\vec{s} = (\cos\theta, \sin\theta)$ is a two-component vector which is constrained to be on the unit circle. The angle θ corresponds to the phase of the order parameter $\psi(\vec{r})$.

In this paper we investigate the x-y model in a film geometry, i.e., planar dimensions L with $L \to \infty$ and a finite thickness H. This study will allow us to examine directly the validity of the FSS theory.

There has been analytical and numerical work on the pure three-dimensional (3D) x-y model. Results of high-temperature-series studies can be found in Ref. 9, Monte Carlo simulations were reported in Refs. 10–13, and a renormalization-group approach based on vortex lines was reported in Ref. 14. In Ref. 15 the anisotropic 3D x-y model ($J_x = J_y \neq J_z$) was studied. A crossover from 3D to two-dimensional (2D) behavior was found with respect to the ratio J_z/J_x. The Villain model, which is in the same universality class as the x-y model, was studied in a film geometry in Ref. 16 where the correlation length in the disordered phase was used to extract the thickness-dependent critical temperature.

In this paper we study the superfluid density or helicity modulus of the x-y model in a film geometry, i.e., on an $L^2 \times H$ lattice. In a film geometry this model exhibits a crossover from 3D to 2D behavior. In the temperature range where the model behaves effectively two dimensionally we are able to compute the values for the helicity modulus in the $L \to \infty$ limit using the Kosterlitz-Thouless-Nelson renormalization-group equations. This enables us to eliminate the L dependence completely and thus to check scaling of the helicity modulus with respect to the film thickness H. We also test further consequences of the FSS theory which are described in the next section. In Sec. III we show how the helicity modulus is computed in our model and briefly describe the Monte Carlo method. Section IV discusses the L dependence of the helicity modulus in the temperature range where the model exhibits two-dimensional behavior. In that section we also describe the extrapolation procedure to the $L = \infty$ limit. In Sec. V we study the scaling of the helicity modulus with respect to H and in Sec. VI we investigate the H dependence of the critical temperature. The last section summarizes our results.

II. X-Y MODEL AND FINITE-SIZE SCALING

The 3D x-y model shows an order-disorder phase transition. Above the bulk critical temperature T_λ, the spin-spin correlation function decays exponentially. The correlation length characterizing this decay grows with the temperature T according to

$$\xi(T) \propto \left(\frac{T - T_\lambda}{T_\lambda}\right)^{-\nu}. \tag{3}$$

In the ordered phase the correlation function decays according to a power law. There, the role of a relevant finite length scale is played by the transverse correlation length,[17] ξ_T. ξ_T, up to a constant factor, is proportional to the ratio T/Υ, where Υ is the helicity modulus. Fisher's scaling hypothesis implies that

$$\xi_T(T) \propto \frac{T}{\Upsilon} \propto \left(\frac{T_\lambda - T}{T_\lambda}\right)^{-\nu}. \tag{4}$$

If the model is considered in a film geometry, i.e., infinite planar dimensions and a finite thickness H, interesting crossover phenomena take place. In Fig. 1 we show an intuitive picture of the behavior of our model with respect to the temperature for a fixed thickness H. Let us start at a temperature far below T_λ where ξ_T is much smaller than the thickness H. At these temperatures the model behaves as a true 3D system. If we raise the temperature in order to approach closer to T_λ from below, the correlation length ξ_T grows according to (4) until we reach the crossover temperature $T_{cr}^- < T_\lambda$ where it becomes comparable to H. Above this temperature the behavior of the system crosses over from 3D to 2D behavior. A further increase in temperature makes the 2D behavior of the system more and more pronounced.

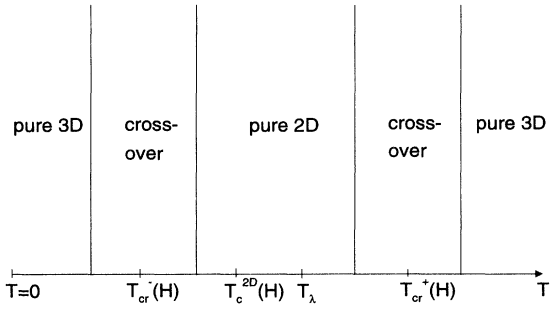

FIG. 1. The behavior of the 3D x-y model in a film geometry for a fixed thickness H with respect to the temperature.

The system starts "feeling" a 2D critical temperature T_c^{2D}. Very close to T_c^{2D}, i.e., in the purely 2D regime, we have to apply the Kosterlitz-Thouless-Nelson theory in order to explain the behavior of the system. This implies that in this regime the correlation length ξ_T does not depend on T according to Eq. (4). Instead, the dimensionless ratio $K = T/(\Upsilon H)$ satisfies the following renormalization-group equations:[18]

$$\frac{dK(l,T)}{dl} = 4\pi^3 y^2(l,T), \tag{5}$$

$$\frac{dy(l,T)}{dl} = [2 - \pi K^{-1}(l,T)]y(l,T). \tag{6}$$

$\ln y$ is the chemical potential to create a single vortex, and e^l denotes the size of the core radius of a vortex. In the limit $l = \infty$—i.e., all vortices have been integrated out—and $T \to T_c^{2D}$ one finds[18]

$$K(l = \infty, T \to T_c^{2D}) = \frac{\pi}{2}\left[1 - b\left(1 - \frac{T}{T_c^{2D}}\right)^{1/2}\right], \tag{7}$$

where b is a constant. $K(l = \infty, T)$ is infinite above T_c^{2D}; i.e., $K(l = \infty)$ exhibits a universal jump at T_c^{2D}. Above T_c^{2D} but still in the purely 2D region, the correlation length grows with T according to the Kosterlitz-Thouless theory, i.e.,

$$\xi_T(T) \propto \exp B/(T - T_c^{2D})^{1/2}, \tag{8}$$

A further increase in temperature results in reaching another crossover temperature T_{cr}^+, where the correlation length ξ_T is comparable to the thickness H. At higher temperatures the model exhibits pure 3D behavior again. From this intuitive picture we deduce the following inequality for the crossover temperatures T_c^{2D} and T_λ:

$$T_{cr}^- < T_c^{2D} < T_\lambda < T_{cr}^+. \tag{9}$$

Within the FSS theory the behavior of our model in the crossover region at temperatures $T \leq T_{cr}^-$ can be described by a universal scaling function Φ which depends only on the ratio $H/\xi_T(T)$, provided H is large enough. According to Ambegaokar *et al.*[19] we have

$$K(T,H) = \frac{T}{\Upsilon(T,H)H} = \Phi(tH^{1/\nu}), \tag{10}$$

where $t = (T_\lambda - T)/T_\lambda$. In the argument of Φ we have replaced $\xi_T(T)$ by its bulk scaling expression (4).

Interesting conclusions can be drawn if we extend the validity of Eq. (10) up to T_c^{2D}.[19] Since $K(T,H)$ drops discontinuously to zero at T_c^{2D}, the scaling function Φ has to be discontinuous too. From the Kosterlitz-Thouless-Nelson theory we have to require

$$\Phi(x < x_c) = \infty,$$
$$\Phi(x_c) = \frac{\pi}{2}. \tag{11}$$

x_c is a dimensionless number. From here we immediately derive an expression for the H dependence of T_c^{2D}, namely,[19]

$$T_c^{2D}(H) = T_\lambda \left(1 - \frac{x_c}{H^{1/\nu}}\right). \tag{12}$$

Equations (7) and (10) have to be reconciled in the two-dimensional region. This enables us to deduce the form of the universal function $\Phi(x)$ for values of x close to x_c. In order to do that we replace T_c^{2D} by T_λ in Eq. (7) by inverting Eq. (12). Keeping only terms linear in $H^{-1/\nu}$ we obtain

$$K(T,H) = \frac{\pi}{2}\left[1 - \frac{b}{H^{1/2\nu}}\left(tH^{1/\nu} + tx_c - x_c - \frac{x_c^2}{H^{1/\nu}}\right)^{1/2}\right]. \tag{13}$$

For T close to T_c^{2D} (i.e., t close to $|1 - T_c^{2D}/T_\lambda|$) we have

$$t \sim \frac{x_c}{H^{1/\nu}}, \tag{14}$$

which yields

$$K(T,H) = \frac{\pi}{2}\left[1 - \frac{b}{H^{1/2\nu}}\left(tH^{1/\nu} - x_c\right)^{1/2}\right]. \tag{15}$$

$K(T,H)$ can only be a universal function of $tH^{1/\nu}$ if b scales according to

$$b(H) = AH^{1/2\nu}; \tag{16}$$

i.e., we obtain

$$\Phi(x) = \frac{\pi}{2}[1 - A(x - x_c)^{1/2}], \tag{17}$$

A is a constant which will be found numerically (see later in the text). The form (17) of the universal function is valid at temperatures very close to T_c^{2D}, since Eq. (7) is only an approximation itself. Petschek[20] uses a different argument in order to derive (16).

III. HELICITY MODULUS AND MONTE CARLO METHOD

The helicity modulus Υ was introduced by Fisher, Barber, and Jasnow.[21] It is related to the superfluid density via[21]

$$\rho_s(T) = \left(\frac{m}{\hbar}\right)^2 \Upsilon(T). \tag{18}$$

For the 3D x-y model on a cubic lattice the definition of the helicity modulus is:[10,22]

$$\frac{\Upsilon_\mu}{J} = \frac{1}{V}\left\langle \sum_{\langle i,j\rangle} \cos(\theta_i - \theta_j)(\vec{e}_\mu \cdot \vec{\epsilon}_{ij})^2 \right\rangle - \frac{\beta}{V}\left\langle \left(\sum_{\langle i,j\rangle} \sin(\theta_i - \theta_j)\vec{e}_\mu \cdot \vec{\epsilon}_{ij} \right)^2 \right\rangle, \tag{19}$$

where V is the volume of the lattice, $\vec{e}_\mu$ is the unit vector in the corresponding bond direction, and $\vec{\epsilon}_{ij}$ is the vector connecting the lattice sites i and j. In the following we will omit the vector index since we will always refer to the x component of the helicity modulus. Note that, because of isotropy, we have $\Upsilon_x = \Upsilon_y$. The above thermal averages denoted by the angular brackets are computed according to

$$\langle O \rangle = Z^{-1} \int \prod_i d\theta_i \, O[\theta] \exp(-\beta\mathcal{H}). \tag{20}$$

$O[\theta]$ denotes the dependence of the physical observable O on the configuration $\{\theta_i\}$, and the partition function Z is given by

$$Z = \int \prod_i d\theta_i \, \exp(-\beta\mathcal{H}), \tag{21}$$

where $\beta = 1/k_B T$. The expectation values (20) are computed by means of the Monte Carlo method using Wolff's one-cluster algorithm.[23] This algorithm successfully tackles the problem of critical slowing down.[24] We computed the helicity modulus on lattices of different sizes $L^2 \times H$, where $H = 3, 4, 6, 8, 10, 12$ and $L = 40, 60, 100$ for each thickness. For some thicknesses we used $L = 25, 50, 100$. Periodic boundary conditions were applied in all directions. We carried out of the order of 10 000 thermalization steps and of the order of 500 000 measurements. The calculations were performed on a heterogenous environment of workstations which include Sun, IBM RS/6000, and DEC alpha AXP workstations and on the Cray-YMP.

IV. TWO-DIMENSIONAL REGION

Here we consider the temperature range $T_{cr}^- < T < T_{cr}^+$, where the 3D bulk correlation length exceeds the thickness of the film. This temperature range contains both the H-dependent 2D critical temperature T_c^{2D} as

well as the 3D bulk critical temperature T_λ. For fixed H and for temperatures close enough to T_c^{2D} the system behaves as a 2D x-y model; thus, our method of analysis applied to the 2D x-y model[25] can be used here as well. In Ref. 25 we investigated the dimensionless quantity Υ/J; in the 3D system the helicity modulus acquires the additional unit of a length^{-1}, and thus the proper quantity to consider is the ratio $\Upsilon(L,H,T)H/J$.

In the following sections we always leave H fixed.

A. Finite-size scaling with respect to L above $T_c^{2D}(H)$

In Fig. 2 we show the data for $\Upsilon(L,H,T)a/J$ for films of fixed thickness $H=6$ for various sizes L and a denotes the lattice spacing. As in Ref. 25 we can obtain a function $T=F(L)$ via the β function such that $\Upsilon(L',H,F(L'))=\Upsilon(L,H,F(L))=\Upsilon_p$, where Υ_p is a physical value of the helicity modulus. We define the β function as

$$\beta(T)=-\lim_{L\to\infty}\frac{dT}{d\ln(L)}. \tag{22}$$

Since we expect our model to behave effectively two dimensionally, we use the ansatz

$$\begin{aligned}\beta[T>T_c(H)]&=c(H)[T-T_c^{2D}(H)]^{1+\nu},\\ \beta[T\le T_c(H)]&=0,\end{aligned} \tag{23}$$

which is suggested by the Kosterlitz-Thouless theory. Inserting the ansatz (23) into (22) and integrating yields

$$\ln L-\frac{B}{[T-T_c(H)]^\nu}=z, \tag{24}$$

where $B=1/(\nu c)$ and z is a constant of integration, which depends on the value of Υ used to define the scaling transformation. As in the pure 2D case we expect all values of $\Upsilon(L,H,T)/J$ for fixed H to collapse on the same universal curve if Υ/J is considered as a function of z. As was explained in Ref. 25 this also means that the correlation length ξ grows according to $\xi(T)\propto\exp B/[T-T_c(H)]^\nu$ because Υ/J for fixed H should be a function of $L/\xi(T)$ only, and thus, also a function of $z=\ln[L/\xi(T)]$. The β function can be found numerically using methods described in Refs. 25–28.

TABLE I. Fitted values of the parameters $c(H)$ and $T_c^{2D}(H)$ of the β function (23) for the used lattice pairs for different thicknesses H; $\nu=0.5$. χ^2 and the goodness of the fit Q are also given.

H	L_1,L_2	c	$T_c^{2D}(H)$	χ^2	Q
3	50,100	0.946(29)	1.7710(23)	0.57	0.92
4	60,100	0.955(41)	1.9039(26)	0.66	0.92
6	50,100	1.383(58)	2.0387(17)	0.55	0.96
8	60,100	1.10(10)	2.0813(31)	0.50	0.98
10	60,100	1.66(18)	2.1182(30)	0.29	1.0

The β function given by Eq. (23) expresses the fact that below the critical temperature $T_c^{2D}(H)$ the correlation length $\xi(T)$ becomes infinite; thus the ratio $L/\xi(T)$ vanishes and the physical quantities are independent of the planar dimensions L of the lattice. For the helicity modulus in particular this means that the values for $\Upsilon(L,H,T)a/J$ for a fixed H computed on different lattices $L\times L\times H$ should collapse onto one curve below the critical temperature $T_c^{2D}(H)$. However, this is not quite true.[25] A close inspection of the curves in Fig. 2 reveals that the pseudocritical temperature $T_c^{2D}(6)$ where the two curves $\Upsilon(25,6,T)a/J$ and $\Upsilon(50,6,T)a/J$ meet is approximately 2.0, whereas

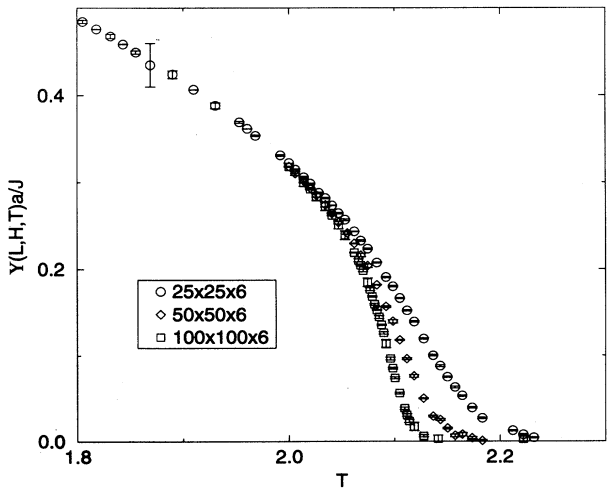

FIG. 2. The helicity modulus $\Upsilon(L,H,T)$ as a function of T for various lattices $L^2\times 6$.

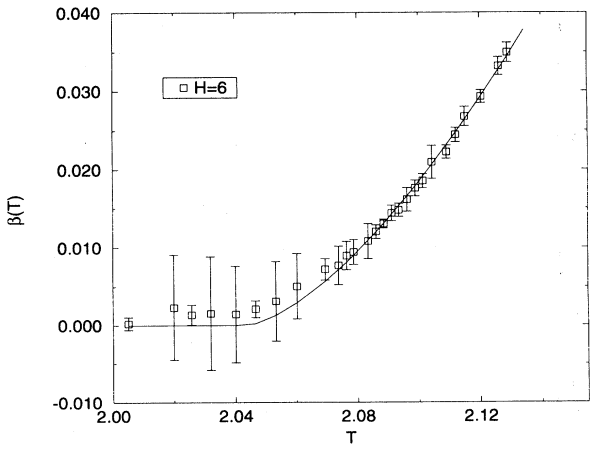

FIG. 3. The β function obtained from the $100^2\times 6$ and $50^2\times 6$ lattices.

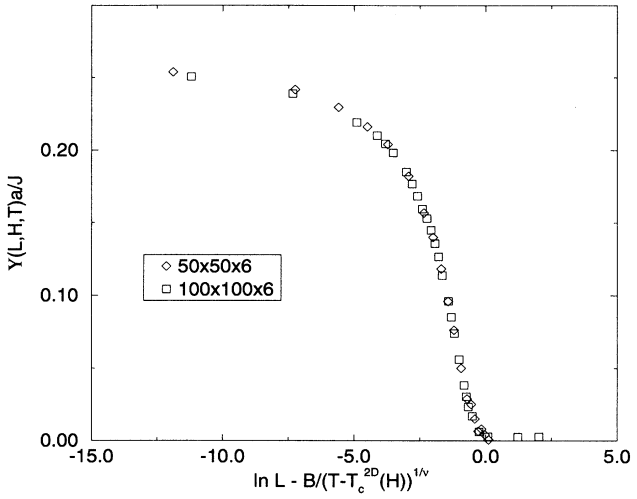

FIG. 4. The helicity modulus Υ as a function of z for the $100^2 \times 6$ and $50^2 \times 6$ lattices.

$T_c^{2D}(6) = 2.0387(17)$ (cf. Table I) is derived from the data for $\Upsilon(50,6,T)a/J$ and $\Upsilon(100,6,T)a/J$; i.e., the estimate for $T_c^{2D}(H)$ grows with L. Solving the Kosterlitz-Thouless-Nelson renormalization-group equations (5) and (6) at the critical critical temperature and for large $l = \ln L$ gives a logarithmic dependence of the critical temperature T_c^{2D} on L.[25] Thus the β-function method can only yield a lower bound for the critical temperature $T_c^{2D}(H)$. Because of this reason, we use the two largest lattices only to numerically derive the β function for each different thickness H. In the next section we will describe and exploit a method that circumvents the difficulties described above.

Having extracted data points for the β function we fit them to the functional form (23) setting $\nu = 0.5$. The results of our fits are given in Table I. Figure 3 shows the β function and Fig. 4 demonstrates that the values for the quantity $\Upsilon a/J$ for the $50^2 \times 6$ and $100^2 \times 6$ lattices collapse onto one curve.

B. Finite-size scaling with respect to L below $T_c^{2D}(H)$

Since our calculation was performed on finite lattices of size $L^2 \times H$, we wish to reach the $L \to \infty$ limit and to obtain $T_c^{2D}(H)$ and $b(H)$ [see Eq. (7)]. In order to do that we need to know the leading finite-L corrections to the dimensionless ratio $K = T/(\Upsilon H)$. As the system behaves effectively two dimensionally we can apply the formulas derived in Ref. 25 for the ratio K. This ratio satisfies the renormalization-group equations (5) and (6); thus solving these equations for a finite scale $l = \ln L$ in the limit $L \to \infty$ and close to the critical temperature $T_c^{2D}(H)$ yields[25]

$$K(L \to \infty, T < T_c(H)) = K_\infty(T)\left(1 + \frac{2[1 - 2K_\infty(T)/\pi]}{1 - \tilde{c}L^{2[\pi/K_\infty(T)-2]}}\right), \quad (25)$$

$$K(L, T_c(H)) = \frac{\pi}{2}\left(1 - \frac{1/2}{\ln L + \tilde{c}'}\right), \quad (26)$$

where $K_\infty(T) \equiv K(L \to \infty, T)$ and $\tilde{c}$ and $\tilde{c}'$ are constants of integration.

At a fixed thickness H below $T_c^{2D}(H)$ we can use the expression (25) to extrapolate our values for $K(L,T)$ at finite L to the values $K_\infty(T)$ at infinite L. In order to do that we fit our calculated values for $K(L,T)$ to the functional form (25). In order to convince ourselves that the values for $K(L,T)$ satisfy Eq. (25) and thus of the justification of the extrapolation method, we computed $K(L, 2.0202)$ for $H = 6$ at $L = 20, 25, 30, 40, 50, 60, 80, 100, 120$ and fitted expression (25) to the obtained values of $K(L, 2.0202)$. The fit is shown in Fig. 5. From the fit we conclude that the data for $K(L, 2.0202)$ follow the functional form (25). Thus we can apply the extrapolation procedure described above. Furthermore, since the data for $K(L,T)$ satisfy Eq. (25), we will restrict ourselves to computing $K(L,T)$ at a given thickness for only three planar lattice extensions L as the functional form (25) contains two parameters which can be determined by a fit to at least three data points. Table II contains our fitting results.

The extrapolated values for $K_\infty(T)$ at a fixed H should behave as[18]

$$K_\infty[T \to T_c^{2D}(H)] = \frac{\pi}{2}\left[1 - b(H)\left(1 - \frac{T}{T_c^{2D}(H)}\right)^{1/2}\right], \quad (27)$$

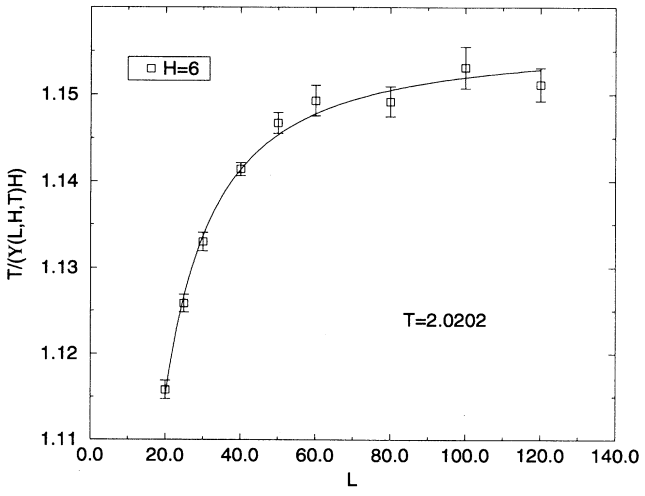

FIG. 5. $T/[\Upsilon(L,H,T)H]$ as a function of L at $T = 2.0202$ and $H = 6$. The solid curve is the fit to (25).

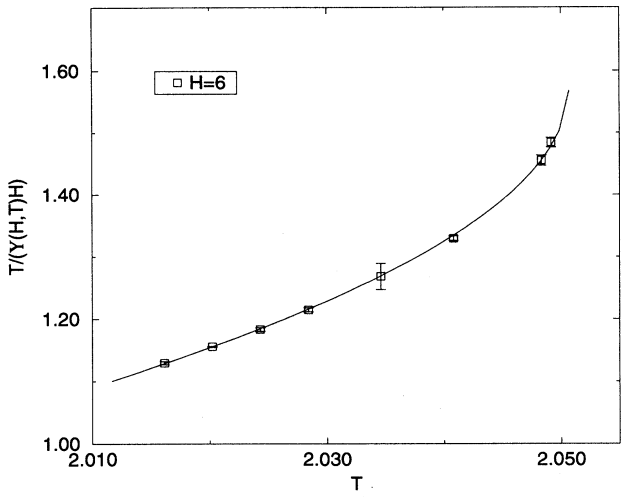

FIG. 6. $T/[\Upsilon(H,T)H]$ at $L=\infty$ and $H=6$ as a function of T. The solid curve is the fit to (27).

TABLE II. Fitted values of the parameters $\tilde{c}$ and $K_\infty(H,T)$ of the expression (25) for various temperatures T and different thicknesses H.

H	T	$\tilde{c}$	$K_\infty(H,T)$
3	1.7699	1.061(33)	1.3363(14)
	1.7544	0.838(55)	1.2691(13)
	1.7391	0.698(30)	1.2150(4)
4	1.9048	0.663(44)	1.2834(20)
	1.8868	0.428(66)	1.1968(20)
	1.8692	0.327(75)	1.1294(9)
6	2.0492	0.912(7)	1.4842(76)
	2.0483	0.862(6)	1.4555(82)
	2.0408	0.566(9)	1.3296(36)
	2.0346	0.396(37)	1.268(21)
	2.0284	0.324(32)	1.2148(33)
	2.0243	0.268(12)	1.1832(29)
	2.0202	0.217(5)	1.1557(8)
	2.0161	0.179(12)	1.1297(26)
8	2.0964	0.433(10)	1.338(12)
	2.0899	0.241(26)	1.2352(52)
	2.0881	0.217(33)	1.2104(63)
	2.0877	0.205(26)	1.2054(52)
	2.0872	0.198(33)	1.1999(67)
10	2.1277	0.518(21)	1.404(12)
	2.1266	0.436(14)	1.359(15)
	2.12653	0.432(14)	1.358(15)
	2.12648	0.429(14)	1.356(14)
	2.12544	0.356(17)	1.318(13)
	2.12540	0.353(17)	1.317(13)
	2.12535	0.351(16)	1.317(12)
12	2.1459	0.596(19)	1.4340(83)
	2.1455	0.516(21)	1.407(11)
	2.1450	0.421(22)	1.387(17)
	2.1445	0.365(24)	1.364(25)
	2.1441	0.317(19)	1.340(37)
	2.1436	0.315(11)	1.330(10)
	2.1432	0.281(9)	1.3109(81)
	2.1427	0.251(10)	1.2962(90)

TABLE III. Fitted values of the parameters $b(H)$ and $T_c^{2D}(H)$ of the expression (27) for different thicknesses H. χ^2 and the goodness of the fit Q are also given.

H	$b(H)$	$T_c^{2D}(H)$	χ^2	Q
3	1.3005(61)	1.7935(5)	0.009	0.92
4	1.5701(94)	1.9310(6)	0.15	0.70
6	2.1672(82)	2.0507(2)	0.48	0.82
8	2.78(10)	2.1023(10)	0.03	0.99
10	3.73(28)	2.1294(5)	0.006	1.0
12	3.91(14)	2.1470(2)	0.02	1.0

where we introduced the expected H dependence of the parameters b and T_c^{2D}. At a fixed H both parameters can be determined by a fit of our results for $K_\infty(T)$ to the functional form (27). The results of our fits are presented in Table III. In Fig. 6 the fit to the data for $K_\infty(T,H)$ at $H=6$ is shown. This fit confirms the validity of Eq. (27). Since the functional form (27) contains two parameters, a fit to three data points gives already an estimate of these parameters. For the films of thickness $H=3,4$ we restricted ourselves to obtaining values for $K_\infty(T,H)$ at only three different temperatures in the temperature range where the system exhibits two-dimensional behavior.

Note that the H dependence of the ratio K is contained in the H dependence of the critical temperature T_c^{2D} and the constant b. These two parameters are the only parameters which are free to depend on the film thickness if we request the form of Eqs. (25), (26), and (27) to be applicable to our case of a film geometry.

We would like to mention one difficulty in extracting the infinite L results $K_\infty(T)$ and finding the parameters $T_c^{2D}(H)$ and $b(H)$. In our study of the pure 2D x-y model[25] we found that formulas (25) and (27) are valid in a narrow interval below T_c^{2D}; in particular the expression (27) is a good approximation for temperatures in the region $\sim 0.9T_c^{2D} \leq T \leq T_c^{2D}$. For films of finite thickness H we have the additional problem of a crossover between 3D and 2D behavior, which makes the region of validity of expression (27) even smaller. Thus, one has to be careful in choosing the correct temperature range for the extrapolation procedure.

V. SCALING OF $T/(\Upsilon H)$ WITH RESPECT TO H

This section is concerned with the scaling relation (10). In order to check the validity of the scaling form (10) we plot first $T/(\Upsilon H)$ versus $tH^{1/\nu}$ using the experimental value of Goldner and Ahlers $\nu=0.6705$ (Ref. 29) and the result of Ref. 13, $T_\lambda=2.2017$. This is done in Fig. 7. In the plot we only use temperatures below $T_c^{2D}(H)$. If the scaling behavior (10) is valid, all our data points should lie on one universal curve. This is not the case for the films of thickness $H=3,4$. For the other films scaling seems valid in the interval $1.0 \leq tH^{1/\nu} \leq 2.4$. All the represented data have lost their L dependence within error bars. Scaling is confirmed by Fig. 8 which

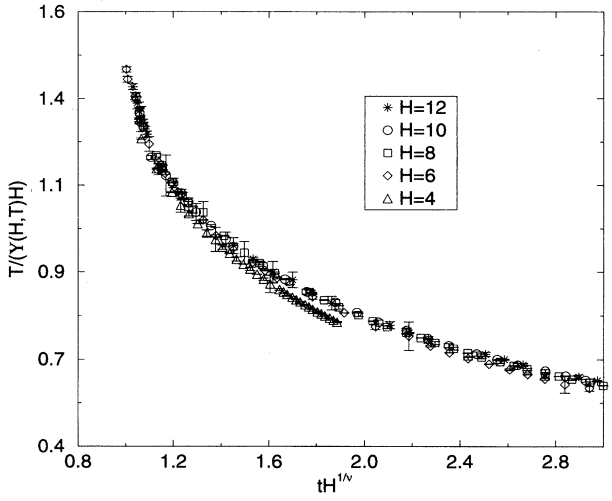

FIG. 7. $T/[\Upsilon(H,T)H]$ as a function of $tH^{1/\nu}$; $\nu = 0.6705$. Only even number thicknesses are displayed.

shows the same plot as Fig. 7, but only the data for the thicknesses $H = 6, 8, 10, 12$ are displayed. The data points collapse onto one universal curve in the specified interval. The films with thickness $H = 3, 4$ are too thin in order to exhibit the scaling behavior (10).

We would like to compare our findings to the experimental results for the superfluid density of very thick films by Rhee, Gasparini, and Bishop (RGB).[3] In our language they plot ΥH versus $tH^{1/\nu}$ and find that their data do not collapse for the expected value of ν. RGB demonstrated the lack of scaling of their data by collapsing them onto one universal curve using a different value of ν [$\nu = 1.14(2)$]. Since we confirm scaling for the ratio $K(T,H)$ in our simulation, the lack of scaling of the experimental data is not due to a breakdown of the phenomenological scaling theory. Note that our results have been obtained with periodic boundary conditions. We are in the process of repeating the calculation using Dirichlet boundary conditions which we believe represent the experimental situation more closely. From these calculations we expect to gain some insight as to why RGB's data do not scale.

Since the scaling function $\Phi(x)$ is known for temperatures which correspond to values of x close to x_c, we can actually find the constants A and x_c in expression (17). For this purpose we plot $K_\infty(H,T)$ given in Table II versus $tH^{1/\nu}$ with the values for T_λ and ν as above for the four thickest films and fit the resulting 28 data points to the form (17). We obtain

$$A = 0.595 \pm 0.002,$$
$$x_c = 0.9965 \pm 0.0009. \tag{28}$$

The fitted curve is the solid line in Fig. 8. The universal function (17) with the parameters (28) describes the collapsed data rather well in the interval $1.0 \leq tH^{1/\nu} \leq 1.3$. Since $T/\Upsilon(T) \propto \xi_T(T)$, we would like to point out that $\Phi(1.3) \sim 1$, i.e., $\xi_T \sim H$. This agrees with the general picture that the 2D behavior sets in when the correlation length exceeds the film thickness.

VI. H DEPENDENCE OF FITTING PARAMETERS

In this section we would like to examine the H dependence of T_c^{2D} and b.

The critical temperatures $T_c^{2D}(H)$ and the parameters $b(H)$ should follow Eq. (12) and Eq. (16), respectively. Since we have determined the numerical values of the pa-

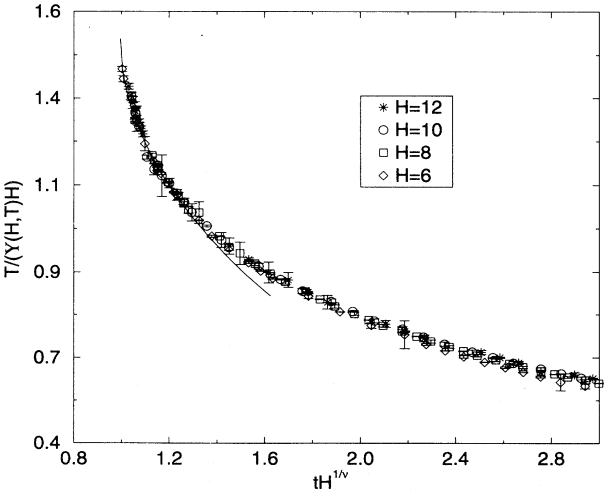

FIG. 8. $T/[\Upsilon(H,T)H]$ as a function of $tH^{1/\nu}$; $\nu = 0.6705$. The solid curve is expression (17) with the parameters (28).

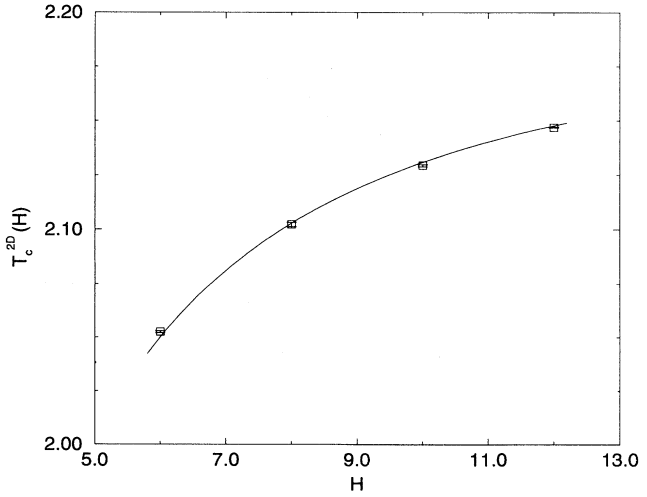

FIG. 9. $T_c^{2D}(H)$ as a function of H. The solid line represents (29).

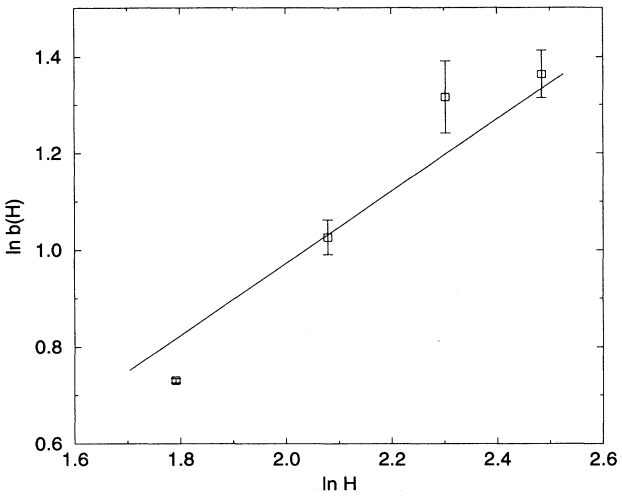

FIG. 10. $\ln b(H)$ as a function of $\ln H$. The solid curve represents (30).

rameters x_c and A [cf. Eq. (28)] in the previous section, we can readily check if the data for $T_c^{2D}(H)$ and $b(H)$ are consistent with the functions

$$T_c^{2D}(H) = 2.2017\left(1.0 - \frac{0.9965}{H^{1.0/0.6705}}\right), \tag{29}$$

and

$$b(H) = 0.595 H^{0.5/0.6705}. \tag{30}$$

In Fig. 9 we plotted the function (29) and the values for the critical temperatures $T_c^{2D}(H)$ for the films which exhibit scaling. Figure 10 shows the curve (30) and the values for $b(H)$. The obtained data for $T_c^{2D}(H)$ agree well with the functional form (29). The agreement of the values for $b(H)$ with the expected curve (30) is not as good as for the values of the critical temperature. However, scaling of the quantity $T/\Upsilon(T,H)$ indicates indirectly that $b(H)$ behaves according to Eq. (16). The fitting parameter $b(H)$ has a much larger error bar than the critical temperature $T_c^{2D}(H)$ (cf. Table III). Therefore more data points in the two-dimensional region than we used are necessary in order to determine $b(H)$ more accurately. We would like to emphasize here that it was not our objective to determine $b(H)$ to a certain accuracy; the main goal of this work was to confirm scaling of the helicity modulus with respect to the film thickness H.

In summary we can state that our results for the critical temperatures $T_c^{2D}(H)$ are in agreement with the expected H dependence, which is deduced from general scaling ideas. The values for the parameter $b(H)$ are consistent with the behavior (16).

VII. SUMMARY

We have investigated the finite-size scaling properties of the superfluid density of a superfluid with respect to the film thickness. This was done by means of a Monte Carlo simulation of the x-y model in a $L\times L\times H$ geometry with periodic boundary conditions in all directions. We extrapolated the values of the superfluid density to the $L\to\infty$ limit in the critical region where the model is effectively two dimensional using the Kosterlitz-Thouless-Nelson renormalization-group equations (5) and (6). The test of the scaling expression (10) revealed that scaling for the quantity $T/\Upsilon(T,H)$ is fulfilled; i.e., the numerical results for this ratio collapse onto one universal curve for sizes of film thickness $H = 6, 8, 10, 12$ used in our Monte Carlo simulation. Furthermore, we derived an analytic expression for the universal curve, which is valid for temperatures close to the critical temperatures of each film. Using the expression (7) we were able to extract the critical temperatures $T_c^{2D}(H)$ and the parameters $b(H)$ entering Eq. (27). The H dependence of the critical temperature agrees with the expected behavior (12) deduced from general scaling arguments. The values for $b(H)$ are consistent with the expected behavior (16). The scaling property of the quantity $T/\Upsilon(T,H)$ demonstrates indirectly the validity of the expected H dependence of $b(H)$.

ACKNOWLEDGMENT

This work was supported by the National Aeronautics and Space Administration under Grant No. NAGW-3326.

[1] D. J. Bishop and J. D. Reppy, Phys. Rev. Lett. **40**, 1727 (1978).
[2] J. Maps and R. B. Hallock, Phys. Rev. Lett. **47**, 1533 (1981).
[3] I. Rhee, F. M. Gasparini, and D. J. Bishop, Phys. Rev. Lett. **63**, 410 (1989).
[4] D. Finotello, Y. Y. Yu, and F. M. Gasparini, Phys. Rev. B **41**, 10 994 (1990).
[5] Y. Y. Yu, D. Finotello, and F. M. Gasparini, Phys. Rev. B **39**, 6519 (1989).
[6] M. E. Fisher and M. N. Barber, Phys. Rev. Lett. **28**, 1516 (1972); M. E. Fisher, Rev. Mod. Phys. **46**, 597 (1974); V. Privman, *Finite Size Scaling and Numerical Simulation of Statistical Systems* (World Scientific, Singapore, 1990).
[7] E. Brezin, J. Phys. (Paris) **43**, 15 (1982).
[8] H. Kleinert, *Gauge Fields in Condensed Matter* (World Scientific, Singapore, 1989).
[9] P. Butera, M. Comi, and A. J. Guttmann, Phys. Rev. B **48**, 13 987 (1993); R. G. Bowers and G. S. Joyce, Phys. Rev. Lett. **19**, 630 (1967); M. Ferer, M. A. Moore, and M. Wortis, Phys. Rev. B **8**, 5205 (1973).
[10] Y.-H. Li and S. Teitel, Phys. Rev. B **40**, 9122 (1989).
[11] G. Kohring, R. E. Shrock, and P. Wills, Phys. Rev. Lett. **57**, 1358 (1986); A. P. Gottlob, M. Hasenbusch, and S.

Meyer, Nucl. Phys. B (Proc. Suppl.) **30**, 838 (1993).
[12] M. Hasenbusch and S. Meyer, Phys. Lett. B **241**, 238 (1990).
[13] W. Janke, Phys. Lett. A **148**, 306 (1992).
[14] G. A. Williams, Phys. Rev. Lett. **59**, 1926 (1987); S. R. Shenoy, Phys. Rev. B **40**, 5056 (1989).
[15] S. T. Chui and M. R. Giri, Phys. Lett. A **128**, 49 (1988); W. Janke and T. Matsui, Phys. Rev. B **42**, 10 673 (1990).
[16] W. Janke and K. Nather, Phys. Rev. B **48**, 15 807 (1993).
[17] P. C. Hohenberg, A. Aharony, B. I. Halperin, and E. D. Siggia, Phys. Rev. B **13**, 2986 (1976).
[18] D. R. Nelson and J. M. Kosterlitz, Phys. Rev. Lett. **39**, 1201 (1977).
[19] V. Ambegaokar, B. I. Halperin, D. R. Nelson, and E. D. Siggia, Phys. Rev. B **21**, 1806 (1980).
[20] R. G. Petschek, Phys. Rev. Lett. **57**, 501 (1986).
[21] M. E. Fisher, M. N. Barber, and D. Jasnov, Phys. Rev. B **16**, 2032 (1977).
[22] S. Teitel and C. Jayaprakash, Phys. Rev. B **27**, 598 (1983).
[23] U. Wolff, Phys. Rev. Lett. **62**, 361 (1989).
[24] U. Wolff, Nucl. Phys. **B322**, 759 (1989); Nucl. Phys. B (Proc. Suppl.) **17**, 93 (1990).
[25] N. Schultka and E. Manousakis, Phys. Rev. B **49**, 12 071 (1994).
[26] P. Harten and P. Suranyi, Nucl. Phys. **B265** [FS15], 615 (1989).
[27] P. Hasenfratz (unpublished).
[28] E. Manousakis, Rev. Mod. Phys. **63**, 1 (1991).
[29] L. S. Goldner and G. Ahlers, Phys. Rev. B **45**, 13 129 (1992).